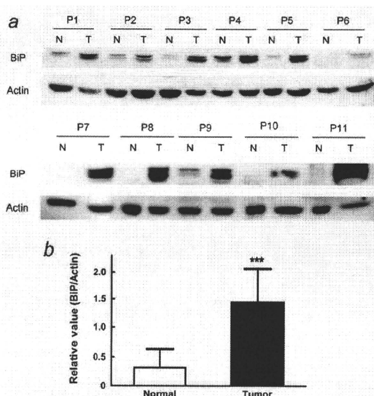


**Figure 7.** BiP expression in human tumor tissues obtained from patients with colon cancer. (*a*) Normal tissues (N) and tumor tissues (T) from 11 patients with colon cancer were homogenized. BiP and actin were detected in the extracted protein samples by Western blot analysis. (*b*) The relative band density (BiP/Actin) was calculated using ImageJ software. The data indicate the mean ± SD ($n$ = 11 patients), ***$p < 0.001$.

stimulated with VEGF. Of those proteins, the expression levels of BiP were highly elevated in the membrane/organelle fraction from angiogenic endothelial cells. Therefore, we focused on BiP and investigated its expression and functions in response to stimulation with VEGF.

BiP is also called GRP78; it belongs to the heat shock protein 70 family and is constitutively expressed in the endoplasmic reticulum (ER) of most cell types.[40] Its expression is shown to be induced by various stresses, such as hypoxia or glucose deprivation,[41] and is elevated in tumor tissues such as breast,[42] gastric,[43] colon[44] and lung.[45] It is also known to function in various biological processes, such as protein folding, maintenance of ER functions, and protection of cells from apoptosis.[46–48] In our experiments, knockdown of BiP expression could suppress VEGF-induced cell proliferation by inhibition of the phosphorylation of ERK1/2, PLCγ and VEGFR-2 in endothelial cells. Recently, it has been shown that BiP/GRP78 heterozygous mice exhibited substantial reductions in tumor microvessel density.[29] Our data support those results and further suggest that the suppression of tumor angiogenesis may be caused by BiP knockdown-induced inhibition of VEGF signal transduction in endothelial cells. Interestingly, our data also suggest that BiP regulates signal transduction in the phosphorylation of VEGFR-2. The regulation of VEGFR-2 strongly suggests that BiP is associated with VEGF-induced angiogenesis. Although certain studies have shown that BiP or other molecular chaperones act with cytoplasm signal mediators, such as Raf-1,[49] the involvement of BiP in receptor tyrosine kinases is largely unknown. Philippova *et al.* demonstrated that BiP interacts with T-cadherin, which is associated with VEGF signal transduction.[50,51] It has also been reported that Cripto (Cripto-1, TDGF1) forms a protein complex with BiP and that the complex is necessary for MAPK signaling in tumors.[52] It is likely that BiP regulates the phosphorylation of VEGFR-2 by forming protein complexes with such molecules on the cell surface.

Nontargeted long circulating liposomes are accumulated in tumors through the enhanced permeability and retention effect; these have been used as drug carriers of cytotoxic agents such as doxorubicin.[53] Active targeting of the liposomes with various ligands may further enhance their activity. Previous studies have demonstrated that tumor endothelium-targeted drug delivery is a useful approach for improving therapeutic efficacy by appending antivascular effect.[19,20] Although BiP is known to be expressed in the ER of most tissues, it has been reported to be expressed on the cell surface in specific conditions such as in cancer cells; however, it is not expressed on cell surfaces in normal organs.[12,14] We showed that the cell surface expression of BiP was increased by VEGF treatment. In addition to our results, BiP expression on endothelial cell surface has also been reported in brain tumors or under hypoxic conditions.[54,55] To deliver cytotoxic agents to the tumor vasculature, we designed liposomes targeting BiP/GRP78. In our study, we have shown that targeting BiP enhances the affinity of liposomes to angiogenic endothelial cells and the therapeutic effects of a liposomal anticancer agent without dramatic toxicity in mice. Since the cancer cells used in the experiments did not exhibit a dramatic uptake of the BiP-targeted liposomes, the obtained results are likely to occur mainly through a vasculature-targeted effect. Thus BiP, a protein identified by proteomic analysis in our study, can be regarded as a novel target molecule for antineovascular therapy. Vasculature disrupting agents, such as combretastatin A-4, selectively impair established tumor vascular networks and lead to various benefits in cancer therapy.[56] Drug delivery of cytotoxic agents is thought to damage tumor endothelial cells as efficiently as do vasculature disrupting agents. BiP-targeting is also shown to be useful in cancer cell-targeted therapy.[27] In our study, we further showed the efficacy of tumor vasculature-targeted drug delivery with BiP. BiP-targeted drug delivery may have a high affinity against both cancer cells and tumor endothelial cells; we consider that it may have certain advantages in cancer therapy.

In conclusion, we have shown the following results: (*i*) BiP may regulate VEGF-induced endothelial cell proliferation through the VEGF-MAPK signal cascade and (*ii*) BiP can be a target molecule for cancer antineovascular therapy. Although further studies are necessary to optimize a BiP-targeted drug delivery tool for clinical use, BiP-targeted cancer therapy may be a possible strategy for anticancer and

antiangiogenic therapy. In contrast to the rapid development of molecular target drugs, few target molecules are available for tumor vasculature-targeted drug delivery. Proteomic approaches may contribute to the further identification of appropriate candidate molecules.


## Acknowledgements

This research was supported by the Center of Excellence (COE) program in the 21st century and Cooperation of Innovative Technology and Advanced Research in Evolutional Area (CITY AREA) to N. Oku and N. Ohashi from the Japanese Ministry of Education, Culture, Sports, Science and Technology.


## References


1. Carmeliet P, Jain RK. Angiogenesis in cancer and other diseases. *Nature* 2000;407: 249–57.
2. Bergers G, Benjamin LE. Tumorigenesis and the angiogenic switch. *Nat Rev Cancer* 2003;3:401–10.
3. Nakao S, Kuwano T, Tsutsumi-Miyahara C, Ueda S, Kimura YN, Hamano S, Sonoda KH, Saijo Y, Nukiwa T, Strieter RM, Ishibashi T, Kuwano M, et al. Infiltration of COX-2-expressing macrophages is a prerequisite for IL-1 beta-induced neovascularization and tumor growth. *J Clin Invest* 2005;115:2979–91.
4. Neri D, Bicknell R. Tumour vascular targeting. *Nat Rev Cancer* 2005;5:436–46.
5. Ferrara N, Gerber HP, LeCouter J. The biology of VEGF and its receptors. *Nat Med* 2003;9:669–76.
6. Ellis LM, Hicklin DJ. VEGF-targeted therapy: mechanisms of anti-tumour activity. *Nat Rev Cancer* 2008;8:579–91.
7. Olsson AK, Dimberg A, Kreuger J, Claesson-Welsh L. VEGF receptor signalling—in control of vascular function. *Nat Rev Mol Cell Biol* 2006;7:359–71.
8. Fujii K, Kondo T, Yokoo H, Yamada T, Iwatsuki K, Hirohashi S. Proteomic study of human hepatocellular carcinoma using two-dimensional difference gel electrophoresis with saturation cysteine dye. *Proteomics* 2005;5:1411–22.
9. Petricoin EF, Zoon KC, Kohn EC, Barrett JC, Liotta LA. Clinical proteomics: translating benchside promise into bedside reality. *Nat Rev Drug Discov* 2002;1: 683–95.
10. Dieguez-Acuna FJ, Gerber SA, Kodama S, Elias JE, Beausoleil SA, Faustman D, Gygi SP. Characterization of mouse spleen cells by subtractive proteomics. *Mol Cell Proteomics* 2005;4:1459–70.
11. Schirmer EC, Florens L, Guan T, Yates JR, III, Gerace L. Nuclear membrane proteins with potential disease links found by subtractive proteomics. *Science* 2003;301: 1380–2.
12. Jang JH, Hanash S. Profiling of the cell surface proteome. *Proteomics* 2003;3: 1947–54.
13. Mayrhofer C, Krieger S, Allmaier G, Kerjaschki D. DIGE compatible labelling of surface proteins on vital cells in vitro and in vivo. *Proteomics* 2006;6:579–85.
14. Shin BK, Wang H, Yim AM, Le Naour F, Brichory F, Jang JH, Zhao R, Puravs E, Tra J, Michael CW, Misek DE, Hanash SM. Global profiling of the cell surface proteome of cancer cells uncovers an abundance of proteins with chaperone function. *J Biol Chem* 2003;278:7607–16.
15. Kerbel RS. A cancer therapy resistant to resistance. *Nature* 1997;390:335–6.
16. Tozer GM, Kanthou C, Baguley BC. Disrupting tumour blood vessels. *Nat Rev Cancer* 2005;5:423–35.
17. Kondo M, Asai T, Katanasaka Y, Sadzuka Y, Tsukada H, Ogino K, Taki T, Baba K, Oku N. Anti-neovascular therapy by liposomal drug targeted to membrane type-1 matrix metalloproteinase. *Int J Cancer* 2004;108:301–6.
18. Maeda N, Takeuchi Y, Takada M, Sadzuka Y, Namba Y, Oku N. Anti-neovascular therapy by use of tumor neovasculature-targeted long-circulating liposome. *J Control Release* 2004;100:41–52.
19. Oku N, Asai T, Watanabe K, Kuromi K, Nagatsuka M, Kurohane K, Kikkawa H, Ogino K, Tanaka M, Ishikawa D, Tsukada H, Momose M, et al. Anti-neovascular therapy using novel peptides homing to angiogenic vessels. *Oncogene* 2002;21: 2662–9.
20. Pastorino F, Brignole C, Marimpietri D, Cilli M, Gambini C, Ribatti D, Longhi R, Allen TM, Corti A, Ponzoni M. Vascular damage and anti-angiogenic effects of tumor vessel-targeted liposomal chemotherapy. *Cancer Res* 2003;63:7400–9.
21. Murphy EA, Majeti BK, Barnes LA, Makale M, Weis SM, Lutu-Fuga K, Wrasidlo W, Cheresh DA. Nanoparticle-mediated drug delivery to tumor vasculature suppresses metastasis. *Proc Natl Acad Sci USA* 2008;105:9343–8.
22. Katanasaka Y, Asai T, Naitou H, Ohashi N, Oku N. Proteomic characterization of angiogenic endothelial cells stimulated with cancer cell-conditioned medium. *Biol Pharm Bull* 2007;30:2300–7.
23. Griffin TJ, Gygi SP, Ideker T, Rist B, Eng J, Hood L, Aebersold R. Complementary profiling of gene expression at the transcriptome and proteome levels in Saccharomyces cerevisiae. *Mol Cell Proteomics* 2002;1:323–33.
24. Fuse C, Ishida Y, Hikita T, Asai T, Oku N. Junctional adhesion molecule-C promotes metastatic potential of HT1080 human fibrosarcoma. *J Biol Chem* 2007;282: 8276–83.
25. Misra UK, Deedwania R, Pizzo SV. Binding of activated alpha2-macroglobulin to its cell surface receptor GRP78 in 1-LN prostate cancer cells regulates PAK-2-dependent activation of LIMK. *J Biol Chem* 2005;280:26278–86.
26. Asai T, Suzuki Y, Matsushita S, Yonezawa S, Yokota J, Katanasaka Y, Ishida T, Dewa T, Kiwada H, Nango M, Oku N. Disappearance of the angiogenic potential of endothelial cells caused by Argonaute2 knockdown. *Biochem Biophys Res Commun* 2008;368:243–8.
27. Arap MA, Lahdenranta J, Mintz PJ, Hajitou A, Sarkis AS, Arap W, Pasqualini R. Cell surface expression of the stress response chaperone GRP78 enables tumor targeting by circulating ligands. *Cancer Cell* 2004;6:275–84.
28. Davidson DJ, Haskell C, Majest S, Kherzai A, Egan DA, Walter KA, Schneider A, Gubbins EF, Solomon L, Chen Z, Lesniewski R, Henkin J. Kringle 5 of human plasminogen induces apoptosis of endothelial and tumor cells through surface-expressed glucose-regulated protein 78. *Cancer Res* 2005;65:4663–72.
29. Dong D, Ni M, Li J, Xiong S, Ye W, Virrey JJ, Mao C, Ye R, Wang M, Pen L, Dubeau L, Groshen S, et al. Critical role of the stress chaperone GRP78/BiP in tumor proliferation, survival, and tumor angiogenesis in transgene-induced mammary tumor development. *Cancer Res* 2008;68:498–505.
30. Takahashi T, Yamaguchi S, Chida K, Shibuya M. A single autophosphorylation site on KDR/Flk-1 is essential for VEGF-A-dependent activation of PLC-gamma and DNA synthesis in vascular endothelial cells. *EMBO J* 2001;20:2768–78.
31. Korbelik M, Sun J, Cecic I. Photodynamic therapy-induced cell surface expression and release of heat shock proteins: relevance for tumor response. *Cancer Res* 2005;65: 1018–26.
32. Sabarth N, Lamer S, Zimny-Arndt U, Jungblut PR, Meyer TF, Bumann D. Identification of surface proteins of *Helicobacter pylori* by selective biotinylation, affinity purification, and two-dimensional gel electrophoresis. *J Biol Chem* 2002;277:27896–902.
33. Maeda N, Takeuchi Y, Takada M, Namba Y, Oku N. Synthesis of angiogenesis-targeted peptide and hydrophobized

polyethylene glycol conjugate. *Bioorg Med Chem Lett* 2004;14:1015–7.
34. Allen TM. Ligand-targeted therapeutics in anticancer therapy. *Nat Rev Cancer* 2002;2: 750–63.
35. Bendardaf R, Buhmeida A, Hilska M, Laato M, Syrjanen S, Syrjanen K, Collan Y, Pyrhonen S. VEGF-1 expression in colorectal cancer is associated with disease localization, stage, and long-term disease-specific survival. *Anticancer Res* 2008;28: 3865–70.
36. Ferrara N, Hillan KJ, Gerber HP, Novotny W. Discovery and development of bevacizumab, an anti-VEGF antibody for treating cancer. *Nat Rev Drug Discov* 2004; 3:391–400.
37. Abe M, Sato Y. cDNA microarray analysis of the gene expression profile of VEGF-activated human umbilical vein endothelial cells. *Angiogenesis* 2001;4:289–98.
38. Pawlowska Z, Baranska P, Jerczynska H, Koziolkiewicz W, Cierniewski CS. Heat shock proteins and other components of cellular machinery for protein synthesis are up-regulated in vascular endothelial cell growth factor-activated human endothelial cells. *Proteomics* 2005;5:1217–27.
39. Abdolzade-Bavil A, Hayes S, Goretzki L, Kroger M, Anders J, Hendriks R. Convenient and versatile subcellular extraction procedure, that facilitates classical protein expression profiling and functional protein analysis. *Proteomics* 2004;4:1397–405.
40. Kim I, Xu W, Reed JC. Cell death and endoplasmic reticulum stress: disease relevance and therapeutic opportunities. *Nat Rev Drug Discov* 2008;7:1013–30.
41. Li J, Lee AS. Stress induction of GRP78/BiP and its role in cancer. *Curr Mol Med* 2006;6:45–54.
42. Fernandez PM, Tabbara SO, Jacobs LK, Manning FC, Tsangaris TN, Schwartz AM, Kennedy KA, Patierno SR. Overexpression of the glucose-regulated stress gene GRP78 in malignant but not benign human breast lesions. *Breast Cancer Res Treat* 2000;59: 15–26.
43. Song MS, Park YK, Lee JH, Park K. Induction of glucose-regulated protein 78 by chronic hypoxia in human gastric tumor cells through a protein kinase C-epsilon/ERK/AP-1 signaling cascade. *Cancer Res* 2001;61:8322–30.
44. Xing X, Lai M, Wang Y, Xu E, Huang Q. Overexpression of glucose-regulated protein 78 in colon cancer. *Clin Chim Acta* 2006;364:308–15.
45. Uramoto H, Sugio K, Oyama T, Nakata S, Ono K, Yoshimastu T, Morita M, Yasumoto K. Expression of endoplasmic reticulum molecular chaperone Grp78 in human lung cancer and its clinical significance. *Lung Cancer* 2005;49:55–62.
46. Di Sano F, Ferraro E, Tufi R, Achsel T, Piacentini M, Cecconi F. Endoplasmic reticulum stress induces apoptosis by an apoptosome-dependent but caspase 12-independent mechanism. *J Biol Chem* 2006; 281:2693–700.
47. Dong D, Ko B, Baumeister P, Swenson S, Costa F, Markland F, Stiles C, Patterson JB, Bates SE, Lee AS. Vascular targeting and antiangiogenesis agents induce drug resistance effector GRP78 within the tumor microenvironment. *Cancer Res* 2005;65: 5785–91.
48. Misra UK, Deedwania R, Pizzo SV. Activation and cross-talk between Akt. NF-kappa. B, and unfolded protein response signaling in 1-LN prostate cancer cells consequent to ligation of cell surface-associated. GRP78. *J Biol Chem* 2006;281: 13694–707.
49. Shu CW, Sun FC, Cho JH, Lin CC, Liu PF, Chen PY, Chang MD, Fu HW, Lai YK. GRP78 and Raf-1 cooperatively confer resistance to endoplasmic reticulum stress-induced apoptosis. *J Cell Physiol* 2008;215:627–35.
50. Philippova M, Banfi A, Ivanov D, Gianni-Barrera R, Allenspach R, Erne P, Resink T. Atypical GPI-anchored T-cadherin stimulates angiogenesis in vitro and in vivo. *Arterioscler Thromb Vasc Biol* 2006; 26:2222–30.
51. Philippova M, Ivanov D, Joshi MB, Kyriakakis E, Rupp K, Afonyushkin T, Bochkov V, Erne P, Resink TJ. Identification of proteins associating with glycosylphosphatidylinositol- anchored T-cadherin on the surface of vascular endothelial cells: role for Grp78/BiP in T-cadherin-dependent cell survival. *Mol Cell Biol* 2008;28:4004–17.
52. Kelber JA, Panopoulos AD, Shani G, Booker EC, Belmonte JC, Vale WW, Gray PC. Blockade of Cripto binding to cell surface GRP78 inhibits oncogenic Cripto signaling via MAPK/PI3K and Smad2/3 pathways. *Oncogene* 2009;28: 2324–36.
53. Maeda H, Wu J, Sawa T, Matsumura Y, Hori K. Tumor vascular permeability and the EPR effect in macromolecular therapeutics: a review. *J Control Release* 2000;65:271–84.
54. Hardy B, Battler A, Weiss C, Kudasi O, Raiter A. Therapeutic angiogenesis of mouse hind limb ischemia by novel peptide activating GRP78 receptor on endothelial cells. *Biochem Pharmacol* 2008; 75:891–9.
55. McFarland BC, Stewart J, Jr, Hamza A, Nordal R, Davidson DJ, Henkin J, Gladson CL. Plasminogen kringle 5 induces apoptosis of brain microvessel endothelial cells: sensitization by radiation and requirement for GRP78 and LRP1. *Cancer Res* 2009;69:5537–45.
56. Kanthou C, Tozer GM. Microtubule depolymerizing vascular disrupting agents: novel therapeutic agents for oncology and other pathologies. *Int J Exp Pathol* 2009;90: 284–94.

# Liposomal Polyamine–Dialkyl Phosphate Conjugates as Effective Gene Carriers: Chemical Structure, Morphology, and Gene Transfer Activity

Takehisa Dewa,*,† Tomohiro Asai,⊥ Yuka Tsunoda,⊥ Kiyoshi Kato,† Daisuke Baba,† Misa Uchida,† Ayumi Sumino,† Kayoko Niwata,⊥ Takuya Umemoto,⊥ Kouji Iida,# Naoto Oku,⊥ and Mamoru Nango*,†

Department of Life and Materials Engineering, Nagoya Institute of Technology, Gokiso-cho, Showa-ku, Nagoya 466-8555 Japan, Department of Medical Biochemistry and Global COE, University of Shizuoka School of Pharmaceutical Sciences, 52-1 Yada, Suruga-ku, Shizuoka, 422-8526 Japan, and Nagoya Municipal Industrial Research Institute, 3-4-41 Rokuban-cho, Atsuta-ku, Nagoya 456-0058 Japan. Received August 24, 2009; Revised Manuscript Received January 5, 2010

Synthetic cationic lipids are promising transfection agents for gene therapy. We report here that polyamine conjugates of dialkyl phosphates, combined with natural lipids and assembled in the form of liposomes (polycationic liposome: PCL), possess high transfection activity in the COS-1 cell line. Furthermore, we describe the functional morphology of the PCL/DNA complexes as revealed by atomic force microscopy (AFM). The conjugates were synthesized from dialkyl phosphates (with alkyl chain lengths of 12, 14, or 16 carbons) by reaction with the polyamine molecules, spermidine, spermine, or polyethylenimine (PEI(1800)). [Dewa, T., et al. *Bioconjugate Chem.* **2004**, *15*, 824]. The PCL composed of the spermidine and C16 conjugate combined with phospholipid and cholesterol (conjugate/phospholipid/cholesterol = 1/1/1 as a molar ratio) exhibited 3.6 times higher activity than that of a popular commercial product. Systematic tests revealed clear correlations of the transgene activity with physical properties of the polyamine, in particular, that longer alkyl chains and the lower molecular weight polyamines (spermidine, spermine) favor high efficacy at the higher nitrogen/phosphate ratio = 24 (N/P, stoichiometric ratio of nitrogen in the conjugate to phosphate in DNA). The low molecular weight polyamine-based PCLs, which formed 150–400 nm particles with plasmid DNA (lipoplexes), exhibited ~3-fold higher gene transfer activity than micellar aggregates (lacking phospholipid and cholesterol) of the corresponding conjugate. In contrast, the PEI-based PCL formed large aggregates (~1 $\mu$m), that, like the micellar aggregate form, had low activity. Activity of the low molecular weight polyamine-based PCLs increased linearly with the N/P of the lipoplex up to N/P = 24. Formation of lipoplexes was examined by agarose gel electrophoresis, dynamic light scattering (DLS), and AFM. At the lower N/P = 5, large aggregates of complex (~1 $\mu$m), in which DNA molecules were loosely packed, were observed. At higher N/P, lipoplexes were converted into smaller particles (150–400 nm) having a lamellar structure, in which DNA molecules were tightly packed. Such morphological features of the lipoplex correlate with the dependence of transfection on the N/P in that the lamellar structures gave superior transfection. AFM also indicated that the lipoplexes disassembled significantly, releasing DNA, when the lipoplexes were exposed to acidic conditions (pH 4). The significance for transfection activity of the metamorphosis of bilayer lipoplexes is discussed relative to that of the less active micellar aggregate form, which is unresponsive to pH change.

## INTRODUCTION

Development of more efficient and safer gene carriers using nonviral compounds is one of the most challenging aspects of gene therapy (*1, 2*). Compared to viral carrier systems, nonviral gene carrier systems have advantages in simplicity of use, lack of specific immune response, and ease of mass production due to the low cost of preparation; however, they have the disadvantage of low transfection efficiency, which needs to be overcome (*3, 4*). To improve the efficiency of nonviral carriers, many synthetic organic compounds, including cationic lipids (*5–9*), polycations (*10–15*), and combinations thereof (*16–22*), have been developed as nonviral gene carriers (*23*). Substantial research has been reported on structure–activity relationships for cationic amphiphiles concerning the cationic and hydrophobic portions (*24–28*). Such amphiphiles form self-assembling micelles and liposomes in an aqueous phase, the structures of which have been investigated using small-angle X-ray scattering (SAXS)[1], transmission electron microscopy (TEM), and atomic force microscopy (AFM) to gain knowledge about structure–activity relationship, particularly those involving ordered structures (lamellar, inverted hexagonal, and cubic phases) and their morphological changes (*29, 30*) as well as about the size of complexes (*31*).

The mechanism of gene delivery by such cationic carriers probably involves an endosomal pathway (*32*): (i) cellular uptake via endocytosis, (ii) DNA release from endosome, and (iii) entry

* To whom correspondence should be addressed. Department of Life and Materials Engineering, Nagoya Institute of Technology, Gokiso-cho, Showa-ku, Nagoya 466-8555 Japan (T.D.) Tel/Fax: +81-52-735-5144. (M.N.) Tel/Fax: +81-52-735-5226. E-mail: takedewa@nitech.ac.jp, nango@nitech.ac.jp.

† Nagoya Institute of Technology.

⊥ University of Shizuoka.

# Nagoya Municipal Industrial Research Institute.

[1] Abbreviations: SAXS, small-angle X-ray scattering: TEM, transmission electron microscopy; AFM, atomic force microscopy; NLS, nuclear localization signal peptide; PCL, polycation liposome; PEI, polyethylenimine; MALDI-TOF-MS, matrix assisted laser desorption ionization-time-of-flight-mass spectroscopy; DOPE, 1,2-dioleoyl-*sn*-glycero-3-phosphoethanolamine; DPPC, 1,2-dipalmitoyl-*sn*-glycero-3-phosphoethanolamine; PLL, poly(L-lysine); FBS, fetal bovine serum; DMEM, Dulbecco's Modified Eagle Medium; N/P, nitrogen/phosphate ratio.

10.1021/bc900376y © 2010 American Chemical Society
Published on Web 04/08/2010

**Scheme 1. Polyamine-Dialkyl Phosphate Conjugates As Gene Carriers**[a]

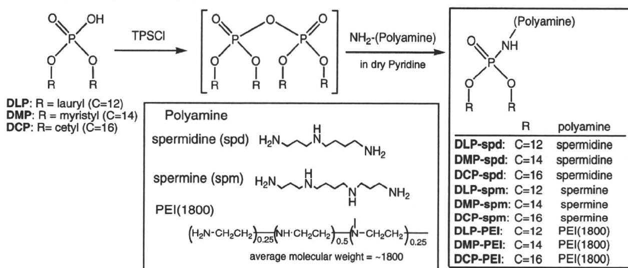


[a] $NH_2$-(Polyamine) represents polyamines and their primary amine portion that reacts with the phosphate portion.

into the nucleus. Many researchers have devised cationic compounds that facilitate the process, for example, ligand-conjugated molecules targeting a receptor such as integrin (*33, 34*), pH-responsive or cleavable molecules that enable escape of DNA from endosome (*13, 35−38*), and conjugation of nuclear localization signal peptides (NLS) (*39, 40*) for steps (i)−(iii), respectively. For cationic lipids/DNA complexes (lipoplexes), it has been proposed that a morphological change from lamellar to inverted hexagonal phase in the acidic endosomal environment facilitates the endosomal release and escape of DNA (*41, 42*). In addition to investigation of intracellular trafficking of polycation−DNA complexes (polyplexes and lipoplexes), observation of morphology and metamorphosis of the complexes is very important to shed light on the mechanism of gene transfer and provide information for development of novel synthetic carriers (*30, 43, 44*).

We have reported that polycationic liposomes (PCL) containing cetylated polyethylenimine (cetyl-PEI) possess high gene transfer activity (*45−47*). The cetyl-PEI molecule is anchored by the hydrophobic cetyl portion and is distributed over the liposomal surface. In our previous report, we proposed a possible mechanism of PCL-mediated gene transfer, in which PCL/DNA complexes are taken up by the endosomal pathway (based on tracking of fluorescence-labeled components, PCL lipid, cetyl-PEI, and DNA), after which the cetyl-PEI/DNA complex is released and transferred into the nucleus via the cytosol (*48*). Compaction of DNA is therefore crucial, and both electrostatic and hydrophobic interactions in the cetyl-PEI/DNA complex are responsible for its effective compaction.

We have previously described novel polyamine (spermidine, spermine, or PEI)-dicetyl phosphate conjugates, prepared via a facile synthetic route (Scheme 1) (*49*) in which the polyamine and phosphate portions are linked through a P−N bond. When suspended in aqueous solution, they form micellar aggregates and exhibit moderate gene-transfer activity, the magnitude of which is relatively insensitive to the modification of the polyamine portion. In the present report, we present (1) evidence demonstrating that the transgene activity is dramatically enhanced when the conjugates are assembled into liposomes containing cholesterol and phospholipid and that the activity is susceptible to the chemical modification of the conjugate both in the polyamine and in the hydrophobic chain portions (Scheme 1). We show further that (2) gene transfer activity of the corresponding PCLs strongly depends on the type of polyamine in the conjugate, with notable differences between the lower molecular weight polyamines (spermidine and spermine) on one hand and the polymer type (PEI(1800)) on the other.

We also examined (3) the morphology of the lipoplexes by AFM and discuss the relationship between the structure of lipoplexes and their transfection efficiency. AFM analysis has a considerable advantage for observation of lipoplex morphology, especially for less ordered structures (*50*); however, until now little clear evidence has been reported on the relationship between morphological change and DNA release. In this research, DNA release as a result of disassociation of the complex was revealed by AFM. We discuss morphology−activity relationships on the basis of electrophoresis analysis, dynamic light scattering (DLS), and AFM observation.

## EXPERIMENTAL PROCEDURES

**General Methods.** Unless stated otherwise, all chemicals and reagents were obtained commercially and used without further purification. Dialkyl phosphates, dilauryl phosphate (DLP), dimyristyl phosphate (DMP), and dicetyl phosphate (DCP) were synthesized from corresponding alcohols, i.e., lauryl (C12), myristyl (C14), and cetyl (C16) alcohols, and $POCl_3$ in accordance with the reported method (*51*). The polyamine−dicetyl phosphate conjugates, DCP-spermidine (**DCP-spd**), DCP-spermine (**DCP-spm**), and DCP-PEI(1800) (**DCP-PEI**) were synthesized as described previously (*49*). Other conjugates, DLP-spermidine (**DLP-spd**), DLP-spermine (**DLP-spm**), DLP-PEI(1800) (**DLP-PEI**), DMP-spermidine (**DMP-spd**), DMP-spermine (**DMP-spm**), and DMP-PEI(1800) (**DMP-PEI**), were also synthesized using analogous procedures. Spectral data are given below. (Note: The asymmetric molecule, spermidine, has two distinguishable primary amines. Products, **DLP-spd**, **DMP-spd**, and **DCP-spd**, bearing a spermidine moiety, have two isomers, which, to date, have not been identified spectroscopically. Similarly, the content of primary amine of PEI(1800) in the products DLP-PEI, DMP-PEI, and DCP-PEI is 25% in total amino moieties (on the basis of theoretical calculation); thus, some structural uncertainty cannot be avoided.)

DLP-spermidine conjugate (**DLP-spd**). $^1$H NMR (300 MHz, $CDCl_3$): $\delta$ 0.88 (t, 6H), 1.26 (s, 36H), 1.51−1.95 (br m, 12H), 2.65−3.05 (br m, 6H), 3.98 (br m, 4H), 4.50 (br s, 4H). MALDI-TOF-MS for $(C_{31}H_{69}N_3O_3P)^+$: calcd 562.9, found 563.0.

DLP-spermine conjugate (**DLP-spm**). $^1$H NMR (300 MHz, $CDCl_3$): $\delta$ 0.88 (t, 6H), 1.26 (s, 36H), 1.49−2.00 (br m, 15H), 2.63−3.05 (br m, 14H), 3.95 (br m, 4H). MALDI-TOF-MS for $(C_{34}H_{76}N_4O_3P)^+$: calcd 620.0, found 620.2.

DLP-PEI(1800) conjugate (**DLP-PEI**). $^1$H NMR (300 MHz, $CDCl_3$): $\delta$ 0.88 (t, 6H), 1.26 (s, 36H), 1.58−1.65 (br m, 4H), 2.55−3.80 (br m, 209H), 3.95 (br m, 4H).

DMP-spermidine conjugate (**DMP-spd**). $^1$H NMR (300 MHz, $CDCl_3$): $\delta$ 0.88 (t, 6H), 1.26 (s, 44H), 1.50−1.71 (br m, 10H), 2.61−3.02 (br m, 12H), 3.98 (br m, 4H). MALDI-TOF-MS for $(C_{35}H_{77}N_3O_3P)^+$: calcd 619.0, found 618.9.

DMP-spermine conjugate (**DMP-spm**). $^1$H NMR (300 MHz, $CDCl_3$): $\delta$ 0.88 (t, 6H), 1.26 (s, 44H), 1.61−2.00 (br m, 17H), 2.63−3.04 (br m, 12H), 3.97 (br m, 4H). MALDI-TOF-MS for $(C_{38}H_{84}N_4O_3P)^+$: calcd 676.1, found 676.1.

DMP-PEI(1800) conjugate (**DMP-PEI**). $^1$H NMR (300 MHz, $CDCl_3$): $\delta$ 0.88 (t, 6H), 1.26 (s, 44H), 1.56−1.65 (br m, 4H), 2.55−3.82 (br m, 209H), 3.95 (br m, 4H).

**Preparation of Polycation Liposome (PCL).** Polycation liposome suspensions were typically prepared as follows: polyamine conjugate, phospholipid (either 1,2-dioleoyl-*sn*-glycero-3-phosphoethanolamine (DOPE) or 1,2-dipalmitoyl-*sn*-glycero-3-phosphocholine (DPPC)), and cholesterol (1/1/1 as a molar ratio) were dissolved in chloroform/*t*-butyl alcohol (2/1). After removal of chloroform under reduced pressure, the residual solvent was removed by freeze−drying overnight. The lyophilized powder was hydrated with Tris-HCl buffer (20 mM, pH 8.0) followed by three freeze−thaw cycles, and the resultant suspension was then subsequently extruded through polycarbonate membranes of 0.4, 0.2, and 0.1 $\mu$m pore diameter at room temperature. For vesicles composed of DPPC, the hydration and extrusion were carried out at 60 °C. Unless stated otherwise, PCL refers to the DOPE-based polycation liposome. A suspension of the polyamine conjugate alone was prepared in the Tris-HCl buffer (20 mM, pH 8.0) by ultrasonication for 3 min. For convenience, particles so prepared are termed "micellar aggregates". Hereafter, polycation liposomes (PCL) and micellar aggregates (M) composed of the conjugates are described as "**conjugate**(PCL)", such as **DCP-spd**(PCL), and "**conjugate**(M)", such as **DCP-spd**(M), respectively.

**Lipoplex Formation with Plasmid DNA.** A plasmid encoding luciferase gene, pCAG-luc3 (6480 bp, a gift of DNAVEC Institute, Tsukuba, Japan), was amplified in *E. coli* JM109 (Nippon Gene, Toyama, Japan) and purified as described before (*47*). One microgram of the plasmid DNA in a TE buffer was added to a suspension of PCL containing 1 mM of polyamine conjugate so as to give the desired nitrogen/phosphate ratio, N/P. The mixture was incubated for 20 min at room temperature when used for transfection. A plasmid, ColE1 DNA (6646 bp, Nippon Gene), was used for an assay of ethidium bromide intercalation and morphological observation of lipoplexes with AFMs (JSPM-4210, JEOL, and PicoPlus, Molecular Imaging), using the AC mode under ambient air conditions. A sample was deposited on a mica surface by spin coating, followed by drying in a desiccator for 1 h under reduced pressure to remove water from the mica surface. A freshly cleaved mica surface is negatively charged. As appropriate, the mica was treated with poly(L-lysine) (PLL) to provide positively charged surface. Hereafter, the negatively and positively charged mica substrates are described as bare mica and PLL-mica, respectively.

The sizes of PCLs, micellar aggregates, and their lipoplexes were analyzed by dynamic light scattering (DLS) with a NICOMP particle sizing system (model 370, Santa Barbara, CA, USA). The $\zeta$-potentials of the cationic vectors were measured with ZETA SIZER Nano-ZS (MALVERN, Worcestershire, U.K.). Agarose-gel electrophoretic analysis was conducted by using 0.8% agarose (UltraPure agarose, Invitrogen) and 1 kb DNA ladder marker (Invitrogen). Electrophoresed DNA bands were stained with ethidium bromide.

For observation of morphological change of lipoplex by acidification, to a solution of lipoplex (pH 8.0) was added acetic acid so as to acidify down to pH 4. The solution was incubated for 1 h at room temperature.

**Transfection Procedure.** COS-1 cells were cultured in Dulbecco's modified Eagle medium (DMEM) supplemented with 10% fetal bovine serum (FBS, Japan Bioserum Co. Ltd.) under a humidified atmosphere of 5% $CO_2$ in air. One day before a transfection experiment, 1 × $10^5$ COS-1 cells were seeded onto each of several 35 mm dishes and incubated overnight in a $CO_2$ incubator. Then, the cells were washed twice with DMEM, and a suspension of lipoplex (1 $\mu$g DNA) was added to them in the presence of 10% FBS-DMEM. After 3 h incubation (37 °C, 5% $CO_2$), the cells were washed twice with DMEM and cultured for another 48 h in 10% FBS-DMEM. The cells in the 35 mm dishes were washed twice with phosphate-buffered saline at 37 °C, and 200 $\mu$L of cell lysis buffer (LC-$\beta$, TOYO B-Net Co. Ltd., Tokyo) was added. After 15 min incubation, the cells were collected with a cell scraper, frozen at −80 °C, and then thawed at room temperature. The lysate was centrifuged at 15 000 rpm for 5 min at 4 °C. The supernatant was subjected to the luciferase assay (Pica Gene, TOYO B-Net Co. Ltd., Tokyo) using a luminophotometer (Luminescencer-PSN AB-2200, ATTO). The observed intensity in instrument light units was normalized to the amount of protein determined by BCA protein assay kit (PIERCE) to give relative light units (RLU/mg protein).

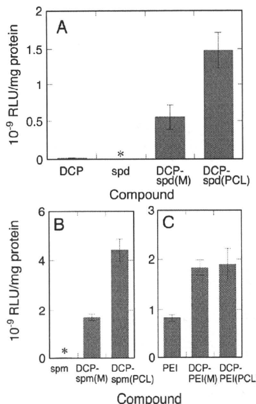


**Figure 1.** Transfection efficacy of polyamine−lipid conjugates, **DCP-spd** (A), **DCP-spm** (B), and **DCP-PEI** (C), and their constituents, DCP (A) and polyamines, spermidine (spd, A), spermine (spm, B), and PEI(1800) (PEI, C), on COS-1 cells. Efficacy was evaluated with the luciferase activity. The observed values for spermidine and spermine indicated by the asterisks (*) were apparently negligible on the activity scale shown. The conjugates **DCP-spd**(M), **DCP-spm**(M), and **DCP-PEI**(M) represent their micellar aggregate forms, and **DCP-spd**(PCL), **DCP-spm**(PCL), and **DCP-PEI**(PCL) represent the conjugate-based PCLs (conjugate/DOPE/cholesterol = 1/1/1 (mol/mol/mol)). The nitrogen/phosphate (N/P) ratio was 16/1 for the polyamine conjugate/DNA complexes. For the monoanionic DCP, the molar ratio, DCP/nucleotide = 16/1, was applied as a negative control experiment. Transfection was conducted in the presence of 10% FBS.

## RESULTS

**Transfection Efficacy of Micellar Aggregates and PCL Vectors: Comparison of the Dicetyl Phosphate Derivatives of Spermidine, Spermine, and Polyamine.** Figure 1A shows the transfection efficacy of the polyamine conjugate, **DCP-spd**(M), and its constituent molecules, DCP and spermidine (spd). The conjugate (in this case an aqueous micellar suspension) shows greatly increased efficacy relative to the constituent molecules, DCP and spermidine. For these polyamine/DNA complexes, the nitrogen/phosphorus ratio (N/P) was 16. The data of the figure indicate that coupling the lipophilic and cationic portions is essential to obtain gene transfer. Such an

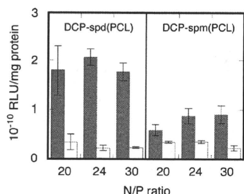


**Figure 2.** Transfection efficacy of spermidine and spermine conjugates (**DCP-spd** and **DCP-spm**, respectively) incorporated into DOPE-based (closed bar) and DPPC-based (open bar) liposomes. Polyamine conjugate/phospholipid/cholesterol = 1/1/1 (mol/mol/mol). Transfection was conducted in the presence of 10% FBS.

effect of conjugating these two moieties was also observed for the spermine conjugate, **DCP-spm**(M) (Figure 1B). When the conjugates were further formulated with DOPE and cholesterol (conjugate/DOPE/cholesterol = 1/1/1 (mol/mol/mol)) to generate polycation liposomes (PCL) (**DCP-spd**(PCL) and **DCP-spm**(PCL)), efficacies were further enhanced by a factor of 2−3 relative to the micellar aggregate suspensions (**DCP-spd**(M) and **DCP-spm**(M)). The polycation PEI(1800) itself showed moderate activity and the conjugate, **DCP-PEI**(M), exhibited even greater activity. However, in contrast to the other conjugates, the activity of the liposomal form, **DCP-PEI**(PCL), was comparable to that of the micellar version, **DCP-PEI**(M). The cytotoxicity of the conjugates, as both micellar aggregates and PCLs, was low; the latter vectors, which exhibited higher activity, also had slightly higher toxicity than the former (Supporting Information Figure S1).

**Effect of the Phospholipid Components of PCLs on Their Transfection Efficacy.** Figure 2 shows the transfection efficacy of **DCP-spd**(PCL) and **DCP-spm**(PCL) composed of either DOPE (dark bar) or DPPC (bright bar) in the N/P range 20−30. It is clear that the DOPE-based PCL exhibits significantly greater activity than the DPPC-based compound for both the **DCP-spd**(PCL) and the **DCP-spm**(PCL). This is indicative of a lipid-mediated gene transfer mechanism; DOPE is well-known as a "helper" lipid, which is believed to facilitate membrane fusion and endosomal escape of the DNA (*52*). DOPE in the present PCL systems presumably also plays a role in the mechanism to expedite membrane fusion and destabilization of the endosomal membrane. DPPC, whose $T_m$ is 41.5 °C (*53*), renders the PCL more stable and more rigid than does DOPE. Thus, it is likely that the fusogenic property of DOPE is responsible for the enhanced transfection activity of its complexes relative to those containing DPPC.

**Optimal Structure of the Conjugate Molecules for Gene Transfer.** The facile synthetic route provides a variety of polycationic compounds that can be exploited to examine the effect of the polycationic and hydrophobic portions on transfection efficiency. We hence examined the effect on transfection activity of different polyamine conjugates incorporated into PCLs: C12, C14, or C16 alkyl chain in the lipophilic portion and spermidine, spermine, or PEI(1800) as the polycationic headgroup of the conjugate. The data on these compounds are shown in Figure 3. This result reveals clear tendencies of longer length of the alkyl group and the lower molecular weight of the polyamines (spermidine, spermine) to enhance transfection. When compared with a commercial product, Lipofectamine 2000, the **DCP-spd**(PCL) possessed 3.6-fold higher activity. The transfection activity of **DCP-spd**(PCL) and **DCP-spm**(PCL) depends on cell lines tested (Figure 3B): **DCP-spd**(PCL) < **DCP-spm**(PCL) for Lewis lung carcinoma (LLC) and **DCP-spd**(PCL) > **DCP-spm**(PCL) for B16BL6.

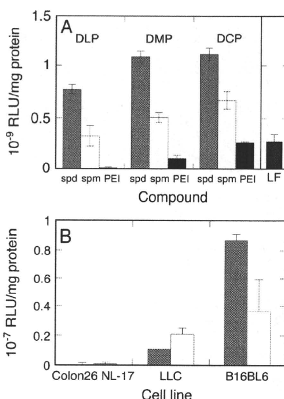


**Figure 3.** (A) Effect of polyamine and hydrophobic portions on PCL-mediated gene transfer efficiency. PCL were composed of polyamine conjugate/DOPE/cholesterol (1/1/1 (mol/mol/mol)). N/P ratio was 24. Transfection was done in the presence of 10% FBS. LF represents Lipofectamine 2000 as a positive control experiment. (B) Transfection efficiency of **DCP-spd**(PCL) (dark bar) and **DCP-spm**(PCL) (open bar) for various murine cancer cells. In the presence of 10% serum, lipoplexes (N/P = 24) were applied to Colon26 NL-17, Lewis lung carcinoma (LLC), and B16BL6 melanoma cells. Transfection procedure was carried out as described in the Experimental Section.

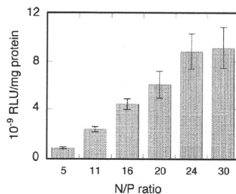


**Figure 4.** Effect of the N/P ratio on the transfection efficacy of **DCP-spm**(PCL) (**DCP-spm**/DOPE/cholesterol = 1/1/1 (mol/mol/mol)). Transfection was in the presence of 10% FBS.

**N/P-Dependent Efficacy and Complexation of PCL with DNA.** Figure 4 shows the dependence of **DCP-spm**(PCL) efficacy on the ratio of the number of nitrogen atoms in the conjugate to that of phosphate in the DNA (N/P). The efficacy increases with the N/P ratio essentially linearly up to 24. A similar N/P dependence has been also observed for **DCP-spd**(PCL) (data not shown for clarity), indicating that excess polyamine relative to DNA is needed for effective gene transfer by PCLs. In contrast, the transfection activity of micellar aggregates **DCP-spd**(M) and **DCP-spm**(M) reaches plateau values in the N/P range 11−16 ($1-2 \times 10^9$ of RLU/mg protein). This tendency is consistent with our previous data obtained with the $\beta$-galactosidase expression system (*49*).

To elucidate the characteristics of N/P dependence, formation of **DCP-spd**(PCL)/DNA and **DCP-spm**(PCL)/DNA lipoplexes was analyzed by agarose gel electrophoreses (Figure 5A,B) and DLS analysis (Table 1). In Figure 5, lane 2 of the plasmid DNA (pCAG-luc3) shows free-DNA bands (supercoiled and open circular DNAs). Lane 3 represents **DCP-spd**(PCL) and **DCP-spm**(PCL) alone as a control experiment. In the lower N/P range

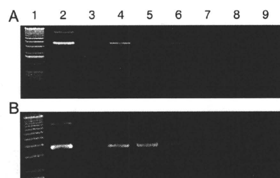


**Figure 5.** Agarose gel electrophoresis of PCL/plasmid DNA (pCAG-luc3: 6480 bp) lipoplexes. **DCP-spd**(PCL) (A) and **DCP-spm**(PCL) (B) were mixed with the DNA in the N/P range 5−30. Lane 1, 1 kb DNA ladder marker; lane 2, plasmid DNA (6480 bp) alone; lane 3, PCL alone. Lanes 4−9 represent PCL/DNA lipoplexes at N/P = 5, 11, 16, 20, 24, and 30, respectively.

**Table 1. DLS Analysis of Various Polyamine-Dialkyl Phosphate Conjugate/DNA Complexes**

| | | | | size (nm) | |
|---|---|---|---|---|---|
| entry | compound | N/P ratio | pH | PCL | micelle |
| 1 | **DCP-spd** | − | 8 | 158 ± 56 | 249 ± 106 |
| 2 | | 2 | 8 | 231 ± 89 | |
| 3 | | 5 | 8 | 651 ± 501 | 1181 ± 1057 |
| 4 | | 16 | 8 | 190 ± 83 | |
| 5 | | 24 | 8 | 261 ± 114 | 1791 ± 1630 |
| 6 | | 24 | 4 | 985 ± 1437 | 1624 ± 1566 |
| 7 | **DCP-spm** | − | 8 | 159 ± 30 | 225 ± 102 |
| 8 | | 2 | 8 | 293 ± 112 | |
| 9 | | 5 | 8 | 764 ± 378 | 321 ± 181 |
| 10 | | 16 | 8 | 296 ± 168 | |
| 11 | | 24 | 8 | 256 ± 116 | 1767 ± 1284 |
| 12 | | 24 | 4 | 1033 ± 1060 | 1209 ± 949 |
| 13 | **DCP-PEI** | − | 8 | 214 ± 90 | 275 ± 184 |
| 14 | | 24 | 8 | 1062 ± 783 | 317 ± 243 |

5−16 (lanes 4−6), the open circular DNA band vanished and the supercoiled DNA band gradually faded for both of **DCP-spd**(PCL) and **DCP-spm**(PCL). In the higher N/P range (20−30, lanes 7−9), the latter DNA band totally disappeared, indicating that the DNA molecules are completely entrapped within the lipoplex. Ethidium bromide (EtBr) replacement experiments also reveal condensation of DNA in the N/P range 5−30 (Supporting Information Figure S2).

The particle size of lipoplexes estimated by DLS analysis is summarized in Table 1. The diameters of the **DCP-spd**(PCL) and **DCP-spm**(PCL) alone are 158 ± 56 and 159 ± 30 nm, respectively (entries 1 and 7). Lipoplexes were larger and their size increased with increasing N/P up to 5 (entries 2 and 8 at N/P = 2 and entries 3 and 9 at N/P = 5). At N/P = 5, the PCL/DNA lipoplexes became larger with a broad distribution from 650 nm to over 1 $\mu$m (entries 3 and 9). In the higher N/P range (N/P = 16−24), sizes were reduced, converging at 261 ± 114 nm (**DCP-spd**(PCL), entry 5) and 256 ± 116 nm (**DCP-spm**(PCL), entry 11). $\zeta$-potential measurements indicated the polarity of surface charge of lipoplexes inverts from negative in the lower N/P (5−11) to positive in the higher N/P (>16) regions.

AFM images revealed characteristic morphologies of lipoplexes in the both low and high N/P ranges (Figure 6A−D). When the **DCP-spd**(PCL)/DNA and **DCP-spm**(PCL)/DNA lipoplexes at N/P = 5 were put on PLL-treated mica (positively charged surface), large aggregates in the sub-micrometer size range (600−1200 nm, Figure 6A,B) were observed. These structures resembled by bead-like aggregates (*54*) composed of small particles (80−120 nm in diameter, 8−20 nm in height) connected to one another. Such aggregates were not observed on a negatively charged bare mica. This is understandable since the lipoplex at N/P = 5 is negatively charged, and the lipoplex must be adsorbed on the PLL-mica surface through electrostatic interaction to be imaged. The outer periphery of the large aggregates is rich in DNA molecules, presumably those were so loosely attached that they were liberated from the aggregates during electrophoresis.

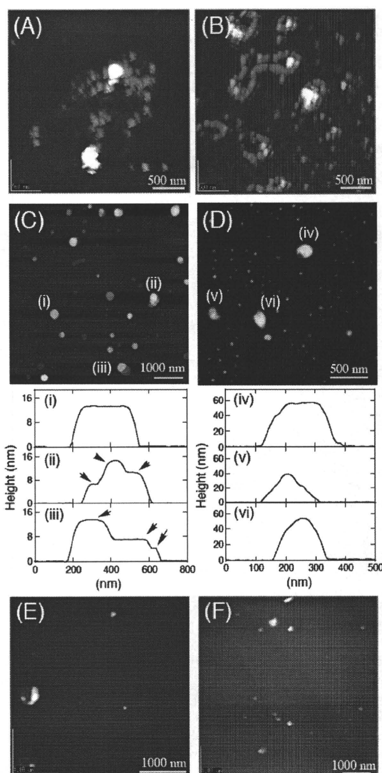


**Figure 6.** AFM images of PCL/plasmid DNA (ColE1; 6646 bp) lipoplexes: (A), **DCP-spd**(PCL)/DNA (N/P = 5); (B), **DCP-spm**(PCL)/DNA (N/P = 5); (C), **DCP-spd**(PCL)/DNA (N/P = 24); (D), **DCP-spm**(PCL)/DNA (N/P = 24); (E and F), **DCP-PEI**(PCL)/DNA complex (N/P = 24). Scale bars shown in the images are 500 nm (A,B,D) and 1000 nm (C,E,F). The PCL/DNA complexes were applied to PLL-mica (A,B) and bare mica (C,D,E,F). All images were taken under an ambient air conditions. Height profiles of the objects (i)−(iii) in C and (iv)−(v) in D are shown below these images. Arrows in (ii) and (iii) indicate step-like profiles discussed in the text. Images E and F for **DCP-PEI**(PCL)/DNA were taken from a different area of the bare mica surface.

At the high N/P = 24, spherical complexes were observed for **DCP-spd**(PCL) and **DCP-spm**(PCL) complexes; their diameters were 200−400 nm for **DCP-spd**(PCL)/DNA (C) and 150−250 nm for **DCP-spm**(PCL)/DNA lipoplexes (D), and their heights were 12−30 and 27−60 nm, respectively. The size of the complexes is in good agreement with the values observed by DLS. The detailed topography of these **DCP-spd**(PCL)/DNA

and **DCP-spm**(PCL)/DNA lipoplexes showed flat-topped spheres and spherical structures (line profiles (i)−(iii) for (C) and (iv)−(vi) for (D)). The profiles (ii) and (iii) are characteristically "step-like" (arrows). The heights indicated in (ii) are 6, 10, and 14 nm. Considering the thickness of lipid bilayer (4 nm) and the diameter of DNA (2 nm), these three values correspond to one bilayer (4 nm) + DNA (2 nm) = 6 nm, a double bilayer (8 nm) + DNA = 10 nm, and a triple bilayer (12 nm) + DNA = 14 nm, respectively. Thus, the step-like structure is reasonably indicative of a smectic lamellar assembly, where DNA molecules are laminated between bilayers.

Compared with **DCP-spd**(PCL) and **DCP-spm**(PCL) lipoplexes, the size of the **DCP-PEI**(PCL)/DNA lipoplex (N/P = 24) is large and has a broad distribution (1062 ± 783 nm, Table 1, entry 14). AFM images of the **DCP-PEI**(PCL)/DNA lipoplex show aggregates with heterogeneous and featureless shapes (Figure 6E,F). EtBr replacement experiments revealed DNA condensation in a similar manner to that of **DCP-spd**(PCL) and **DCP-spm**(PCL) (Supporting Information Figure S2).

**Disruption of the PCL/DNA Lipoplexes.** When the **DCP-spd**(PCL)/DNA and **DCP-spm**(PCL)/DNA lipoplexes (N/P = 24) were incubated in acidic solution (down to pH 4), the particle sizes measured by DLS became significantly larger and exhibited broad distributions (Table 1, entries 6 and 12). AFM imaging revealed morphological transformation of the PCL/DNA complexes upon acidification. When the dispersion of **DCP-spd**(PCL)/DNA lipoplexes (N/P = 24) was acidified at pH 4 for 1 h by addition of acetic acid, deformed structures were observed on bare mica (Figure 7A). Relative to the original structure (Figure 6C), the complex is decisively deformed by the acid treatment. Although some of the flat-topped sphere complexes remain, the predominant morphology is particles connected with strings. The height of the clusters is 25−53 nm and they are connected with string portions that are 6−10 nm high. When the acid-treated complex solution was put on PLL-mica, additional deformed objects appeared on the surface (Figure 7B). A "beads on a string" deformed structure is composed of very small particles (50−100 nm in diameter) and string parts (~70 nm in width and 2−5 nm in height). The beads on a string structure observed on the positively charged surface must consist of DNA-rich fragments associated with some lipid components. The **DCP-spm**(PCL)/DNA lipoplex maintains its spherical structure on bare mica (Figure 7C). On the PLL-mica, on the other hand, deformed structures were observed as in the case of **DCP-spm**(PCL)/DNA lipoplex (Figure 7D). Such morphological changes upon acidification result from disassembly of the lipoplexes and the accompanying DNA release. Gel electrophoretic analysis provided evidence for the DNA release; the released plasmid band increased with the acidification from pH 8 to pH 4 (Supporting Information Figure S4). In sharp contrast, such a morphological change was not observed for the micellar aggregate **DCP-spd**(M) (Figure 7E,F). DLS analysis indicates an insensitivity of the micellar aggregates to acidification (Table 1, entries 6 and 12).

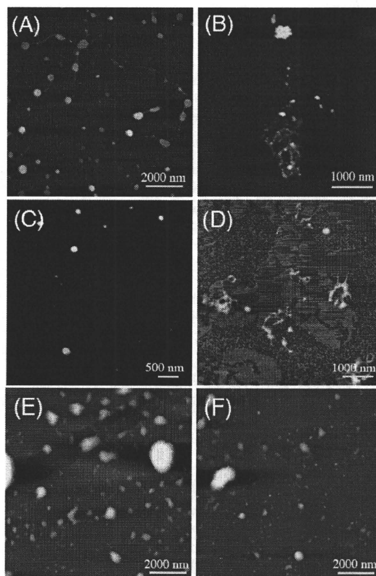


**Figure 7.** AFM images of disassembled lipoplexes, **DCP-spd**(PCL)/DNA (A and B) and **DCP-spm**(PCL)/DNA (C and D) by acidification at pH 4. Images (E) and (F) represent the micellar aggregate **DCP-spd**(M)/DNA complex before and after the acid treatment, respectively. The acid-treated suspensions of complexes were put on bare mica (A,C,E,F) and PLL-mica (B,D). After removal of the solution, the images were acquired. Scale bars: 2000 nm (A), 1000 nm (B), 500 nm (C), 1000 nm (D), 2000 nm (E) and (F).

## DISCUSSION

**Chemical Structure of the Polyamine Conjugates.** The polyamine-dialkyl phosphate conjugates can be readily synthesized via a two-step reaction: (i) formation of dimerized dialkyl phosphate anhydride and (ii) its nucleophilic substitution with polyamines. The synthetic strategy gives access to a wide variety of polyamine−dialkyl phosphate derivatives. Conjugation of the polyamine and hydrophobic portions is required for an effective gene carrier (Figure 1). Such amphiphilicity is essential to condense DNA molecules, which requires both electrostatic and hydrophobic interactions (*45, 49*). We tested a number of combinations of dialkyl and polyamine portions for their activity in gene transfection. The longer alkyl chain exhibited higher efficiency (Figure 3). The ζ-potential of the DOPE-based PCL increased with alkyl chain length, for example, 27.6, 33.4, and 37.1 mV for **DLP-spd, DMP-spd,** and **DCP-spd**, respectively, showing that the conjugate with the longer chain length provides the higher positive potential. The hydrophobic interaction results in stable incorporation of the conjugate into the PCL, consistent with transfection activity in the order of C16 ≥ C14 > C12. We found that the micellar aggregate of **DCP-PEI** conjugate exhibited slightly higher transfection activity than the low-molecular-weight amine conjugates, **DCP-spd**(M) and **DCP-spm**(M); however, the activity of **DCP-PEI**(PCL) was marginal. The size of **DCP-PEI**(PCL)/DNA lipoplex is significantly greater than that of the other lipoplexes (Table 1, entry 14). The **DCP-PEI** conjugate is composed of DCP/PEI(1800) = ~1/1, judged by $^{1}$H NMR (*49*). As previously reported, the cetyl-PEI, whose PCL possesses high transfection activity, consists of 10 cetyl portions in the polymer (*47*). The cetyl-PEI can attach to the PCL surface via the anchoring of cetyl portions in the lipid bilayer. However, that is not the case for **DCP-PEI**(PCL); the single hydrophobic portion in the conjugate is not enough to provide adequate covering of PEI over the PCL surface. This may cause "PEI-protrusion" from the surface, which gives rise to the large and heterogeneous aggregation seen upon combination with DNA molecules. This is likely the reason for the lower activity of the **DCP-PEI**(PCL). Taken together, these consid-

erations suggest that a homogeneous positive charge distribution on the PCL surface is important to the transfection activity.

**Effect of Bilayer Structure on the Transfection Activity.** In the series of polyamines tested in this study, the low-molecular-weight polyamines were found to be more effective gene carriers when these conjugates were assembled into PCLs. The transfection activity of the PCL was ~3 times larger than as the corresponding micellar aggregate (Figure 1). The effect of the helper lipid, DOPE, was clearly substantial, as is shown in Figure 2. DOPE, a predominantly nonlamellar lipid, is thought to facilitate fusion and destabilization of the endosomal membrane after uptake of cationic lipid/DNA complexes into a cell. In our previous report, we described intercellular trafficking of PCL (composed of cetyl-PEI and DOPE)-DNA complexes, which were taken up into cells by endosomal pathway (*48*), followed by endosomal escape. In fact, transfection activity of the present PCLs was inhibited by nigericin, which is able to dissipate the pH gradient across the endosomal membranes, by 30−50%, suggesting that endosomal pathway is likely involved in the mechanism in the present lipoplex system. It appears, therefore, that the mechanism of the lipofection by the compounds in this study may be similar to that of this and other agents known to be enhanced by DOPE. The lipoplexes made from the bilayer-structured PCLs evidently involve lamellar assemblies, given that AFM images reveal the presence of step-like profiles ((ii) and (iii) in Figure 6). The step-like profiles imply a lamellar complex, in which DNA rods (2 nm in diameter) are laminated between bilayers (4 nm thickness). Such an intrinsic bilayer structure may predispose lipoplexes to interact with cell and endosomal membranes. This is not the case for micellar aggregates, whose morphology is large spheres (Figure 7E and Table 1 entry 5), in which polyamine conjugate and DNA molecules likely aggregate randomly. This may be one of the reasons for the higher activity of PCL-based lipoplex, whose size is more favorable to transfection.

The linear dependence of activity on N/P (Figure 4) is related to the morphology of the lipoplex. The electrophoresis experiment (Figure 5) and AFM images (Figure 6A−D) suggest a reasonable explanation of the dependence, namely, the following: In the low N/P range (~5), the PCLs inadequately condense DNA molecules, giving the bead-like structures (Figure 6A,B). The DNA molecules loosely packed in the complex are readily released during electrophoresis. Such a complex, whose $\zeta$-potential is negative, is too large to be introduced into the cell membrane via endocytosis; therefore, the transfection level is low. With increasing N/P ratio, the morphology of the lipoplex transforms from large bead-like structure into smaller particles, wherein DNA molecules are condensed more tightly (Figure 6C,D). The size of the lipoplexes, whose $\zeta$-potential is positive, is 150−400 nm, more favorable for cellular uptake via endocytosis (*30*). Given that the lamellar assembly in the lipoplex is responsible for its effectiveness as a gene carrier (*29, 30*), the population of active species for gene transfer would increase with increasing in the N/P. Although highly positive-charged carriers are generally toxic, the PCL described here exhibit low cytotoxicity, an advantage for in vitro and in vivo applications.

**Disassembly of the Lipoplexes and DNA Release.** Facile escape from the acidic endosomal compartment is necessary for efficient gene transfer. Disassembly of the lipoplex associated with DNA release has been clearly observed by AFM imaging (Figure 7) and by electrophoretic analyses (Supporting Information Figure S3). Upon acidification (down to pH 4), the extent of protonation of the polyamine portion is increased. Assuming that the lipoplex forms smectic lamella, electrostatic repulsion between layers must be increased with such protonation, resulting in the disruption of the lipoplex. For lipoplexes composed of **DCP-spd**(PCL) and **DCP-spm**(PCL), disruption accompanying DNA release has been confirmed. In sharp contrast, the size and shape of micellar aggregate/DNA complexes composed of **DCP-spd** and **DCP-spm** are insensitive to acidification (Figure 7F and Table 1, entries 6 and 12). This would be due to their amorphous structure, which does not respond to pH change. Thus, the disassembly of the lipoplex composed of the bilayer-structured PCL is essential in effective gene transfer, especially in the process of endosomal escape, where lipid exchange and flip−flop are involved in disrupting the membrane and leading to DNA release (*42*). Although the acidity of this experimental condition (pH 4) seems higher than that in endosome (pH 5.5), such a protonation process on the polyamines should be involved in the endosomal environment, because the protonation on the polyamines whose $pK_a$ values are >8 may proceed rather gradually in the acidic region, especially in the self-assembled lamellar structure, where polyamines are densely packed. This finding suggests a strategy for molecular design—especially in the polyamine portion—in which a morphological transformation of lipoplexes is taken advantage of for new nonviral transfection strategies.

## CONCLUSION

We have demonstrated that PCL composed of the low-molecular-weight polyamine conjugates, DCP-spermidine (**DCP-spd**) and DCP-spermine (**DCP-spm**), exhibit much higher gene transfer activity than PEI(1800) conjugate-based **DCP-PEI**(PCL). The former compounds generate 150−400 nm diameter lipoplexes, whereas the latter gives rise to large aggregates. In the case of the former compounds, AFM images clearly reveal a morphological change upon acidification, indicating DNA release from the lipoplexes, whereas in contrast, the morphology of micellar aggregates is insensitive to pH change. A pH-dependent transformation is crucial in gene transfer, and the chemical structure of the polyamine portion may therefore play an important role in the acidification-induced transformation. We have also described the relation between the N/P dependence of transfection activity and the morphology of the lipoplexes as revealed by AFM. Morphological study with AFM provided useful information for understanding the basis of lipoplexes with superior activity and for design strategies leading to optimally efficient gene carriers.

## ACKNOWLEDGMENT

The authors thank Dr. Robert C. MacDonald for helpful comments and discussion. The present work was partially supported by "Grant-in-Aid for Scientific Research on Innovative Areas 2006 (Molecular Science of Fluctuations toward Biological Functions)" (21107510) from the Ministry of Education, Culture, Sports, Science and Technology (MEXT) of the Japanese Government.

**Supporting Information Available:** Evaluation of cytotoxicity polyamine conjugates and their PCLs (Figure S1), changes in fluorescence intensity of ethidium bromide intercalated into ColE1 plasmid DNA-PCLs (Figure S2), and electrophoretic analysis of DNA release from the lipoplex (Figure S3). This material is available free of charge via the Internet at http://pubs.acs.org.

## LITERATURE CITED

(1) Kay, M. A., Liu, D., and Hoogerbrugge, P. M. (1997) Gene therapy. *Proc. Natl. Acad. Sci. U.S.A. 94*, 12744–12746.
(2) Lasic, D. D. (1997) *Liposomes in Gene Derivary*, CRC Press, New York.
(3) Miller, A. D. (1998) Cationic liposomes for gene therapy. *Angew. Chem., Int. Ed. 37*, 1768–1785.

(4) Li, S., and Huang, L. (2000) Nonviral gene therapy: promises and challenges. *Gene Ther. 7*, 31–34.

(5) Felgner, P. L., and Ringold, G. M. (1989) Cationic liposome-mediated transfection. *Nature 337*, 387–388.

(6) MacDonald, R. C., Ashley, G. W., Shida, M. M., Rakhmanova, V. A., Tarahovsky, Y. S., Pantazatos, D. P., Kennedy, M. T., Pozharski, E. V., Baker, K. A., Jones, R. D., Rosenzweig, H. S., Choi, K. L., Qiu, R., and McIntosh, T. J. (1999) Physical and biological properties of cationic triesters of phosphatidylcholine. *Biophys. J. 77*, 2612–2629.

(7) Felgner, P. L., Gadek, T. R., Holm, M., Roman, R., Chan, H. W., Wenz, M., Northrop, J. P., Ringold, G. M., and Danielsen, M. (1987) Lipofection: A highly efficient, lipid-mediated DNA-transfection procedure. *Proc. Natl. Acad. Sci. U.S.A. 84*, 7413–7417.

(8) Behr, J.-P., Demeneix, B., Loeffler, J. P., and Perez-Mutul, J. (1989) Efficient gene transfer into mammalian primary endocrine cells with lipopolyamine-coated DNA. *Proc. Natl. Acad. Sci. U.S.A. 86*, 6982–6986.

(9) Meyer, O., Kirpotin, D., Hong, K., Sternberg, B., Park, J. W., Woodle, M. C., and Papahadjopoulos, D. (1998) Cationic liposomes coated with polyethylene glycol as carriers for oligonucleotides. *J. Biol. Chem. 273*, 15621–15627.

(10) Boussif, O., Lezoulch, F., Zanta, M. A., Mergny, M. D., Scherman, D., Demeneix, B., and Behr, J.-P. (1995) A versatile vector for gene and oligonucleotide transfer into cells in culture and in vivo: Polyethylenimine. *Proc. Natl. Acad. Sci. U.S.A. 92*, 7297–7301.

(11) Petersen, H., Fechner, P. M., Martin, A. L., Kunath, K., Stolnik, S., Roberts, C. J., Fischer, D., Davies, M. C., and Kissel, T. (2002) Polyethylenimine-graft-poly(ethylene glycol) copolymers: influence of copolymer block structure on DNA complexation and biological activities as gene delivery system. *Bioconjugate Chem. 13*, 845–854.

(12) Koide, A., Kishimura, A., Osada, K., Jang, W.-D., Yamasaki, Y., Kataoka, K., Harada, A., and Nagasaki, Y. (2006) Semipermeable polymer vesicle (PICsome) self-assembled in aqueous medium from a pair of oppositely charged block copolymers: Physiologically stable micro-/nanocontainers of water-soluble macromolecules. *J. Am. Chem. Soc. 128*, 5988–5989.

(13) Russ, V., Elfberg, H., Thoma, C., Kloeckner, J., Ogris, M., and Wagner, E. (2008) Novel degradable oligoethylenimine acrylate ester-based pseudodendrimers for in vitro and in vivo gene transfer. *Gene Ther. 15*, 18–29.

(14) Haensler, J., and Szoka, F. C., Jr. (1993) Polyamidoamine cascade polymers mediate efficient transfection of cells in culture. *Bioconjugate Chem. 4*, 372–379.

(15) Shim, M. S., and Kwon, Y. J. (2009) Acid-responsive linear polyethylenimine for efficient, specific, and biocompatible siRNA delivery. *Bioconjugate Chem. 20*, 488–499.

(16) Guillot-Nieckowski, M., Joester, D., Stöhr, M., Losson, M., Adrian, M., Wagner, B., Kansy, M., Heinzelmann, H., Pugin, R., Diederich, F., and Gallani, J.-L. (2007) Self-assembly, DNA complexation, and pH response of amphiphilic dendrimers for gene transfection. *Langmuir 23*, 737–746.

(17) Wu, J., Lizarzaburu, M. E., Kurth, M. J., Liu, L., Wege, H., Zern, M. A., and Nantz, M. H. (2001) Cationic lipid polymerization as a novel approach for constructing new DNA delivery agents. *Bioconjugate Chem. 12*, 251–257.

(18) Ewert, K. K., Evans, H. M., Zidovska, A., Bouxsein, N. F., Ahmad, A., and Safinya, C. R. (2006) A columnar phase of dendritic lipid-based cationic liposome-DNA complexes for gene delivery: Hexagonally ordered cylindrical micelles embedded in a DNA honeycomb lattice. *J. Am. Chem. Soc. 128*, 3998–4006.

(19) Takahashi, T., Hirose, J., Kojima, C., Harada, A., and Kono, K. (2007) Synthesis of poly(amidoamine) dendron-bearing lipids with poly(ethylene glycol) grafts and their use for stabilization of nonviral gene vectors. *Bioconjugate Chem. 18*, 1163–1169.

(20) Matsui, K., Sando, S., Sera, T., Aoyama, Y., Sasaki, Y., Komatsu, T., Terashima, T., and Kikuchi, J. (2006) Cerasome as an infusible, cell-friendly, and serum-compatible transfection agent in a viral size. *J. Am. Chem. Soc. 128*, 3114–3115.

(21) Mustapa, M. F. M., Grosse, S. M., Kudsiova, L., Elbs, M., Raiber, E.-A., Wong, J. B., Brain, A. P. R., Armer, H. E. J., Warley, A., Keppler, M., Ng, T., Lawrence, M. J., Hart, S. L., Hailes, H. C., and Tabor, A. B. (2009) Stabilized integrin-targeting ternary LPD (Lipopolyplex) vectors for gene delivery designed to disassemble within the target cell. *Bioconjugate Chem. 20*, 518–532.

(22) Kogure, K., Akita, H., Yamada, Y., and Harashima, H. (2008) Multifunctional envelope-type nano device (MEND) as a non-viral gene delivery system. *Adv. Drug Delivery Rev. 60*, 559–571.

(23) Mintzer, M. A., and Simanek, E. E. (2009) Nonviral vectors for gene delivery. *Chem. Rev. 109*, 259–302, Also references citied therein.

(24) Remy, J.-S., Sirlin, C., Vierling, P., and Behr, J.-P. (1994) Gene transfer with a series of lipophilic DNA-binding molecules. *Bioconjugate Chem. 5*, 647–654.

(25) Geall, A. J., Eaton, M. A. W., Baker, T., Catterall, C., and Blagbrough, I. S. (1999) The regiochemical distribution of positive charges along cholesterol polyamine carbamates plays significant roles in modulating DNA binding affinity and lipofection. *FEBS Lett. 459*, 337–342.

(26) Ewert, K., Ahmad, A., Evans, H. M., Schmidt, H.-W., and Safinya, C. R. (2002) Efficient synthesis and cell-transfection properties of a new multivalent cationic lipid for nonviral gene delivery. *J. Med. Chem. 45*, 5023–5029.

(27) Byk, G., Dubertret, C., Escriou, V., Frederic, M., Jaslin, G., Rangara, R., Pitard, B., Crouzet, J., Wils, P., Schwartz, B., and Scherman, D. (1998) Synthesis, activity, and structure-activity relationship studies of novel cationic lipids for DNA transfer. *J. Med. Chem. 41*, 224–235.

(28) McGregor, C., Perrin, C., Monck, M., Camilleri, P., and Kirby, A. J. (2001) Rational approaches to the design of cationic gemini surfactants for gene delivery. *J. Am. Chem. Soc. 123*, 6215–6220.

(29) Koltover, I., Salditt, T., Rädler, J. O., and Safinya, C. R. (1998) An inverted hexagonal phase of cationic liposome-DNA complexes related to DNA release and delivery. *Science 281*, 78–81.

(30) Koynova, R., Wang, L., and MacDonald, R. C. (2006) An intracellular lamellar-nonlamellar phase transition rationalizes the superior performance of some cationic lipid transfection agents. *Proc. Natl. Acad. Sci. U.S.A. 103*, 14373–14378.

(31) Aoyama, Y., Kanamori, T., Nakai, T., Sasaki, T., Horiuchi, S., Sando, S., and Niidome, T. (2003) Artificial viruses and their application to gene delivery. Size-controlled gene coating with glycocluster nanoparticles. *J. Am. Chem. Soc. 125*, 3455–3457.

(32) Wrobel, I., and Collins, D. (1995) Fusion of cationic liposomes with mammalian cells occurs after endocytosis. *Biochim. Biophys. Acta 1235*, 296–304.

(33) Mustapa, M. F. M., Bell, P. C., Hurley, C. A., Nicol, A., Guénin, E., Sarkar, S., Writer, M. J., Barker, S. E., Wong, J. B., Pilkington-Miksa, M. A., Papahadjopoulos-Sternberg, B., Shamlou, P. A., Hailes, H. C., Hart, S. L., Zicha, D., and Tabor, A. B. (2007) Biophysical characterization of an integrin-targeted lipopolyplex gene delivery vector. *Biochemistry 46*, 12930–12944.

(34) Varga, C. M., Wickham, T. J., and Lauffenburger, D. A. (2000) Receptor-mediated targeting of gene delivery vectors: Insights from molecular mechanisms for improved vehicle design. *Biotechnol. Bioeng. 70*, 593–605.

(35) Oupicky, D., Parker, A. L., and Seymour, L. W. (2002) Laterally stabilized complexes of DNA with linear reducible polycations: Strategy for triggered intracellular activation of DNA delivery vectors. *J. Am. Chem. Soc. 124*, 8–9.

(36) Dauty, E., Remy, J.-S., Blessing, T., and Behr, J.-P. (2001) Dimerizable cationic detergents with a low cmc condense plasmid DNA into nanometric particles and transfect cells in culture. *J. Am. Chem. Soc. 123*, 9227–9234.

(37) Miyata, K., Kakizawa, Y., Nishiyama, N., Harada, A., Yamasaki, Y., Koyama, H., and Kataoka, K. (2004) Block catiomer polyplexes with regulated densities of charge and disulfide cross-linking directed to enhance gene expression. *J. Am. Chem. Soc. 126*, 2355–2361.

(38) Anderson, D. G., Lynn, D. M., and Lange, R. (2003) Semi-automated synthesis and screening of a large library of degradable cationic polymers for gene delivery. *Angew. Chem., Int. Ed. 42*, 3153–3158.

(39) Zanta, M. A., Beleguise-Valladier, P., and Behr, J.-P. (1999) Gene delivery: A single nuclear localization signal peptide is sufficient to carry DNA to the cell nucleus. *Proc. Natl. Acad. Sci. U.S.A. 96*, 91–96.

(40) Manickam, D. S., and Oupicky, D. (2006) Multiblock reducible copolypeptides containing histidine-rich and nuclear localization sequences for gene delivery. *Bioconjugate Chem. 17*, 1395–1403.

(41) Bell, Paul C., Bergsma, M., Dolbnya, I. P., Bras, W., Stuart, M. C. A., Rowan, A. E., Feiters, M. C., and Engberts, J. B. F. N. (2003) Transfection mediated by gemini surfactants: Engineered escape from the endosomal compartment. *J. Am. Chem. Soc. 125*, 1551–1558.

(42) Xu, Y., and Szoka, F. C., Jr. (1996) Mechanism of DNA release from cationic liposome/DNA complexes used in cell transfection. *Biochemistry 35*, 5616–5623.

(43) Wan, L., Manickam, D. S., Oupicky, D., and Mao, G. (2008) DNA release dynamics from reducible polyplexes by atomic force microscopy. *Langmuir 24*, 12474–12482.

(44) Tarahovsky, Y. S., Koynova, R., and MacDonald, R. C. (2004) DNA release from lipoplexes by anionic lipids: Correlation with lipid mesomorphism, interfacial curvature, and membrane fusion. *Biophys. J. 87*, 1054–1064.

(45) Yamazaki, Y., Nango, M., Matsuura, M., Hasegawa, Y., Hasegawa, M., and Oku, N. (2000) Polyamine liposomes, a novel nonviral gene transfer system, constructed drom cetylated polyethyleninine. *Gene Ther. 7*, 1148–1155.

(46) Oku, N., Yamazaki, M., Matsuura, M., Sugiyama, M., Hasegawa, M., and Nango, M. (2001) A novel non-viral gene transfer system, polycation liposomes. *Adv. Drug Delivery Rev. 52*, 209–218.

(47) Matsuura, M., Yamazaki, Y., Sugiyama, M., Kondo, M., Ori, H., Nango, M., and Oku, N. (2003) Polycation liposome-mediated gene transfer in vivo. *Biochim. Biophys. Acta 1612*, 136–143.

(48) Sugiyama, M., Matsuura, M., Takeuchi, Y., Kosaka, J., Nango, M., and Oku, N. (2004) Possible mechanism of polycation liposome (PCL)-mediated gene transfer. *Biochim. Biophys. Acta 1660*, 24–30.

(49) Dewa, T., Ieda, Y., Morita, K., Wang, L., MacDonald, R. C., Iida, K., Yamashita, K., Oku, N., and Nango, M. (2004) Novel polyamine-dialkyl phosphate conjugates for gene carriers. Facile synthetic route via an unprecedented dialkyl phosphate. *Bioconjugate Chem. 15*, 824–830.

(50) Oberle, V., Bakowsky, U., Zuhorn, I. S., and Hoekstra, D. (2000) Lipoplex formation under equilibrium conditions reveals a three-step mechanism. *Biophys. J. 79*, 1447–1454.

(51) Kunitake, T., and Okahata, Y. (1978) Synthetic bilayer membranes with anionic head groups. *Bull. Chem. Soc. Jpn. 51*, 1877–1879.

(52) Felgner, J. H., Kumar, R., Sridhar, C. N., Wheeler, C. J., Tsai, Y. J., Border, R., Ramsey, P., Martin, M., and Felgner, P. L. (1994) Enhanced gene delivery and mechanism studies with a novel series of cationic lipid formulations. *J. Biol. Chem. 269*, 2550–2561.

(53) Cevc, G. (1993) *Phospholipids Handbook*, Marcel Dekker, Inc., New York.

(54) Yoshikawa, Y., Emi, N., Kanbe, T., Yoshikawa, K., and Saito, H. (1996) Folding and aggregation of DNA chains induced by complexation with lipospermine: formation of a nucleosome-like structure and network assembly. *FEBS Lett. 396*, 71–76.

BC900376Y